SLAC–PUB–7674
January 1997

Measurement of the B^+ and B^0 Lifetimes using Topological Reconstruction of Inclusive and Semileptonic Decays*

The SLD Collaboration

Stanford Linear Accelerator Center,
Stanford University, Stanford, CA 94309

Abstract

The lifetimes of B^+ and B^0 mesons are measured using a sample of 150,000 hadronic Z^0 decays collected by the SLD experiment at the SLC between 1993 and 1995. Two analyses are presented in which the decay length and charge of the B meson are reconstructed. The first method uses a novel topological vertexing technique while the second uses semi-inclusively reconstructed semileptonic decays. The topological analysis yields a sample of 6033 (3665) charged (neutral) vertices with good charge purity, whereas the semileptonic analysis yields a smaller sample of 634 (584) charged (neutral) decays with excellent charge purity. Combining the results from both analyses, we find $\tau_{B^+} = 1.66 \pm 0.06(\text{stat}) \pm 0.05(\text{syst})$ ps, $\tau_{B^0} = 1.64 \pm 0.08(\text{stat}) \pm 0.08(\text{syst})$ ps, and $\tau_{B^+}/\tau_{B^0} = 1.01 \pm 0.07(\text{stat}) \pm 0.06(\text{syst})$.

Submitted to *Physical Review Letters*

*Work supported in part by the Department of Energy contract DE–AC03–76SF00515.

K. Abe,[19] K. Abe,[30] T. Akagi,[28] N.J. Allen,[4] W.W. Ash,[28]†
D. Aston,[28] K.G. Baird,[16] C. Baltay,[34] H.R. Band,[33] M.B. Barakat,[34]
G. Baranko,[9] O. Bardon,[15] T. L. Barklow,[28] G.L. Bashindzhagyan,[18]
A.O. Bazarko,[10] R. Ben-David,[34] A.C. Benvenuti,[2] G.M. Bilei,[22]
D. Bisello,[21] G. Blaylock,[16] J.R. Bogart,[28] B. Bolen,[17] T. Bolton,[10]
G.R. Bower,[28] J.E. Brau,[20] M. Breidenbach,[28] W.M. Bugg,[29]
D. Burke,[28] T.H. Burnett,[32] P.N. Burrows,[15] W. Busza,[15]
A. Calcaterra,[12] D.O. Caldwell,[5] D. Calloway,[28] B. Camanzi,[11]
M. Carpinelli,[23] R. Cassell,[28] R. Castaldi,[23][a] A. Castro,[21]
M. Cavalli-Sforza,[6] A. Chou,[28] E. Church,[32] H.O. Cohn,[29]
J.A. Coller,[3] V. Cook,[32] R. Cotton,[4] R.F. Cowan,[15] D.G. Coyne,[6]
G. Crawford,[28] A. D'Oliveira,[7] C.J.S. Damerell,[25] M. Daoudi,[28]
R. De Sangro,[12] R. Dell'Orso,[23] P.J. Dervan,[4] M. Dima,[8]
D.N. Dong,[15] P.Y.C. Du,[29] R. Dubois,[28] B.I. Eisenstein,[13] R. Elia,[28]
E. Etzion,[33] S. Fahey,[9] D. Falciai,[22] C. Fan,[9] J.P. Fernandez,[6]
M.J. Fero,[15] R. Frey,[20] K. Furuno,[20] T. Gillman,[25] G. Gladding,[13]
S. Gonzalez,[15] E.L. Hart,[29] J.L. Harton,[8] A. Hasan,[4] Y. Hasegawa,[30]
K. Hasuko,[30] S. J. Hedges,[3] S.S. Hertzbach,[16] M.D. Hildreth,[28]
J. Huber,[20] M.E. Huffer,[28] E.W. Hughes,[28] H. Hwang,[20] Y. Iwasaki,[30]
D.J. Jackson,[25] P. Jacques,[24] J. A. Jaros,[28] A.S. Johnson,[3]
J.R. Johnson,[33] R.A. Johnson,[7] T. Junk,[28] R. Kajikawa,[19]
M. Kalelkar,[24] H. J. Kang,[26] I. Karliner,[13] H. Kawahara,[28]
H.W. Kendall,[15] Y. D. Kim,[26] M.E. King,[28] R. King,[28] R.R. Kofler,[16]
N.M. Krishna,[9] R.S. Kroeger,[17] J.F. Labs,[28] M. Langston,[20]
A. Lath,[15] J.A. Lauber,[9] D.W.G.S. Leith,[28] V. Lia,[15] M.X. Liu,[34]

X. Liu,[6] M. Loreti,[21] A. Lu,[5] H.L. Lynch,[28] J. Ma,[32]
G. Mancinelli,[22] S. Manly,[34] G. Mantovani,[22] T.W. Markiewicz,[28]
T. Maruyama,[28] H. Masuda,[28] E. Mazzucato,[11] A.K. McKemey,[4]
B.T. Meadows,[7] R. Messner,[28] P.M. Mockett,[32] K.C. Moffeit,[28]
T.B. Moore,[34] D. Muller,[28] T. Nagamine,[28] S. Narita,[30]
U. Nauenberg,[9] H. Neal,[28] M. Nussbaum,[7] Y. Ohnishi,[19]
L.S. Osborne,[15] R.S. Panvini,[31] C.H. Park,[27] H. Park,[20] T.J. Pavel,[28]
I. Peruzzi,[12][b] M. Piccolo,[12] L. Piemontese,[11] E. Pieroni,[23]
K.T. Pitts,[20] R.J. Plano,[24] R. Prepost,[33] C.Y. Prescott,[28]
G.D. Punkar,[28] J. Quigley,[15] B.N. Ratcliff,[28] T.W. Reeves,[31]
J. Reidy,[17] P.L. Reinertsen,[6] P.E. Rensing,[28] L.S. Rochester,[28]
P.C. Rowson,[10] J.J. Russell,[28] O.H. Saxton,[28] T. Schalk,[6]
R.H. Schindler,[28] B.A. Schumm,[6] S. Sen,[34] V.V. Serbo,[33]
M.H. Shaevitz,[10] J.T. Shank,[3] G. Shapiro,[14] D.J. Sherden,[28]
K.D. Shmakov,[29] C. Simopoulos,[28] N.B. Sinev,[20] S.R. Smith,[28]
M.B. Smy,[8] J.A. Snyder,[34] P. Stamer,[24] H. Steiner,[14] R. Steiner,[1]
M.G. Strauss,[16] D. Su,[28] F. Suekane,[30] A. Sugiyama,[19] S. Suzuki,[19]
M. Swartz,[28] A. Szumilo,[32] T. Takahashi,[28] F.E. Taylor,[15]
E. Torrence,[15] A.I. Trandafir,[16] J.D. Turk,[34] T. Usher,[28] J. Va'vra,[28]
C. Vannini,[23] E. Vella,[28] J.P. Venuti,[31] R. Verdier,[15] P.G. Verdini,[23]
D.L. Wagner,[9] S.R. Wagner,[28] A.P. Waite,[28] S.J. Watts,[4]
A.W. Weidemann,[29] E.R. Weiss,[32] J.S. Whitaker,[3] S.L. White,[29]
F.J. Wickens,[25] D.A. Williams,[6] D.C. Williams,[15] S.H. Williams,[28]
S. Willocq,[28] R.J. Wilson,[8] W.J. Wisniewski,[28] M. Woods,[28]
G.B. Word,[24] J. Wyss,[21] R.K. Yamamoto,[15] J.M. Yamartino,[15]

X. Yang,[20] J. Yashima,[30] S.J. Yellin,[5] C.C. Young,[28] H. Yuta,[30]
G. Zapalac,[33] R.W. Zdarko,[28] and J. Zhou,[20]

(The SLD Collaboration)

[1] *Adelphi University, Garden City, New York 11530*
[2] *INFN Sezione di Bologna, I-40126 Bologna, Italy*
[3] *Boston University, Boston, Massachusetts 02215*
[4] *Brunel University, Uxbridge, Middlesex UB8 3PH, United Kingdom*
[5] *University of California at Santa Barbara, Santa Barbara, California 93106*
[6] *University of California at Santa Cruz, Santa Cruz, California 95064*
[7] *University of Cincinnati, Cincinnati, Ohio 45221*
[8] *Colorado State University, Fort Collins, Colorado 80523*
[9] *University of Colorado, Boulder, Colorado 80309*
[10] *Columbia University, New York, New York 10027*
[11] *INFN Sezione di Ferrara and Università di Ferrara, I-44100 Ferrara, Italy*
[12] *INFN Lab. Nazionali di Frascati, I-00044 Frascati, Italy*
[13] *University of Illinois, Urbana, Illinois 61801*
[14] *Lawrence Berkeley Laboratory, University of California, Berkeley, California 94720*
[15] *Massachusetts Institute of Technology, Cambridge, Massachusetts 02139*
[16] *University of Massachusetts, Amherst, Massachusetts 01003*
[17] *University of Mississippi, University, Mississippi 38677*
[18] *Moscow State University, Institute of Nuclear Physics 119899 Moscow, Russia*
[19] *Nagoya University, Chikusa-ku, Nagoya 464 Japan*
[20] *University of Oregon, Eugene, Oregon 97403*
[21] *INFN Sezione di Padova and Università di Padova, I-35100 Padova, Italy*

[22] *INFN Sezione di Perugia and Università di Perugia, I-06100 Perugia, Italy*
[23] *INFN Sezione di Pisa and Università di Pisa, I-56100 Pisa, Italy*
[24] *Rutgers University, Piscataway, New Jersey 08855*
[25] *Rutherford Appleton Laboratory, Chilton, Didcot, Oxon OX11 0QX United Kingdom*
[26] *Sogang University, Seoul, Korea*
[27] *Soongsil University, Seoul, Korea 156-743*
[28] *Stanford Linear Accelerator Center, Stanford University, Stanford, California 94309*
[29] *University of Tennessee, Knoxville, Tennessee 37996*
[30] *Tohoku University, Sendai 980 Japan*
[31] *Vanderbilt University, Nashville, Tennessee 37235*
[32] *University of Washington, Seattle, Washington 98195*
[33] *University of Wisconsin, Madison, Wisconsin 53706*
[34] *Yale University, New Haven, Connecticut 06511*
[†] *Deceased*
[a] *Also at the Università di Genova*
[b] *Also at the Università di Perugia*

The spectator model predicts that the lifetime of a heavy hadron depends upon the properties of the constituent weakly decaying heavy quark Q and is independent of the remaining, or spectator, quarks in the hadron. This model fails for the charm hadron system where the lifetime hierarchy $\tau_{D^+} \sim 2\tau_{D_s^+} \sim 2.5\tau_{D^0} \sim 5\tau_{\Lambda_c^+}$ is observed. Since corrections to the spectator model are predicted to scale with $1/m_Q^2$ the B meson lifetimes are expected to differ by less than 10% [1]. Hence a measurement of the B^+ and B^0 lifetimes provides a test of this prediction. In addition, the specific B meson lifetimes are needed for precise determinations of the element V_{cb} of the CKM matrix.

Most measurements of the B^+ and B^0 lifetimes [2] are based on samples of semileptonic decays in which the lepton is identified and a $D^{(*)}$ meson is fully reconstructed. Fully exclusive[3] or inclusive[4] techniques have also been used. Except for the inclusive technique, the efficiencies are typically small. In this Letter, we present two complementary analyses that exploit the excellent 3-D vertexing capabilities of SLD to reconstruct the B meson decay length and measure its charge directly with high efficiency. The first analysis uses a novel topological vertexing technique [5] to identify B hadron decay vertices. The decay length is measured using the reconstructed vertex location while the B hadron charge is determined from the total charge of the tracks associated with the vertex. This inclusive technique is very efficient since most B decay modes are used. The second analysis identifies the B hadron charge by reconstructing the charged track topology of both B and cascade D vertices in semileptonic B decays. This technique has lower efficiency but benefits from an increased charge reconstruction purity. In contrast to previous measurements based on semileptonic decays, these

two analyses do not rely on assumptions concerning the B^+ and B^0 content of $\overline{D^0}Xl^+\nu$ and $D^{(*)-}Xl^+\nu$ samples, rather they only rely on the simple difference of total charge between B^+ and B^0 decays.

The measurements presented here are based on a sample of 150,000 hadronic Z^0 decays collected between 1993 and 1995 by the SLD experiment at the SLC and use the tracking and calorimetry systems (for details see Ref. [6]). Tracking is provided by the Central Drift Chamber (CDC) for charged track reconstruction and momentum measurement and the CCD pixel Vertex Detector (VXD) for precise position measurements near the interaction point. These systems are immersed in the 0.6 T field of the SLD solenoid. Charged tracks reconstructed in the CDC are linked with pixel clusters in the VXD by extrapolating each track and selecting the best set of associated clusters[6]. For a typical track from the primary vertex or heavy hadron decay, the total efficiency of reconstruction in the CDC and linking to a correct set of VXD hits is 94% for the region $|\cos\theta| < 0.74$. The track impact parameter resolutions at high momentum are 11 μm and 38 μm in the $r\phi$ and rz projections respectively (z points along the beam direction), while multiple scattering contributions are $70\,\mu\text{m}\,/(p\,\sin^{3/2}\theta)$ in both projections (where the momentum p is expressed in GeV/c). The Liquid Argon Calorimeter (LAC) is used to reconstruct jets from energy clusters and perform electron identification with maximal efficiency for $|\cos\theta| < 0.72$. The Warm Iron Calorimeter (WIC) provides efficient muon identification for $|\cos\theta| < 0.60$.

The decay length is measured relative to the position of the micron-size SLC Interaction Point (IP) which is reconstructed in the $r\phi$ plane with a

precision of $\sigma_{r\phi} = (7 \pm 2)\,\mu$m using tracks in sets of ~ 30 sequential hadronic Z^0 decays. The z position of the IP is determined on an event-by-event basis with $\sigma_z \simeq 52\,\mu$m for $b\,\bar{b}$ events [6] using the median z position of tracks at their point-of-closest-approach to the IP in the $r\phi$ plane.

The measurements rely on a Monte Carlo simulation based on the JETSET 7.4 event generator [7] and the GEANT 3.21 detector simulation package [8] to determine the charge separation purity and to extract the lifetimes from the decay length distributions. The b-quark fragmentation follows the Peterson *et al.* parameterization [9]. B mesons (baryons) are generated with mean lifetime $\tau = 1.55$ ps ($\tau = 1.10$ ps). B meson decays are modelled according to the CLEO B decay model [10] tuned by SLD to reproduce the spectra and multiplicities of leptons, charm hadrons, pions, kaons, and protons, measured at the $\Upsilon(4S)$ [11, 12]. Semileptonic decays follow the ISGW model [13] including 23% D^{**} production. B baryon and charm hadron decays are modelled using JETSET with, in the latter case, branching fractions tuned to existing measurements [14].

We first describe the topological analysis. Hadronic Z^0 event selection is based on the measurements from the tracking and calorimetry systems, and is detailed in Ref. [6]. The selected sample consists of $\sim 96,000$ hadronic Z^0 decays with thrust axis satisfying $|\cos\theta| < 0.71$ (VXD acceptance).

Good quality tracks used for vertex finding must have a CDC hit at a radius<39 cm, and have $\geq$40 hits to ensure that the lever arm provided by the CDC is appreciable. The CDC tracks must have p_T >400 MeV/c and extrapolate to within 1 cm of the IP in $r\phi$ and within 1.5 cm in z to eliminate tracks which arise from interaction with the detector material. The fit of the

track must satisfy χ^2/d.o.f.< 5. At least one good VXD link is required, and the combined CDC/VXD fit must also satisfy χ^2/d.o.f.< 5.

The topological vertex reconstruction is applied separately to the tracks in each hemisphere (defined with respect to the event thrust axis). This analysis is the first application of the algorithm described in detail in Ref. [5] and summarized here. Vertices are reconstructed in 3-D co-ordinate space by defining a vertex function $V(\vec{r})$ at each position $\vec{r}$. The helix parameters for each track i are used to describe the 3-D track trajectory as a Gaussian tube $f_i(\vec{r})$, where the width of the tube is the uncertainty in the measured track location close to the IP. A function $f_0(\vec{r})$ is used to describe the location and uncertainty of the IP. $V(\vec{r})$ is defined as a function of $f_0(\vec{r})$ and the $f_i(\vec{r})$ such that it is large in regions of high track multiplicity. Maxima are found in $V(\vec{r})$ and clustered into resolved spatial regions. Tracks are associated with these regions to form a set of topological vertices.

The efficiency for reconstructing B hadron decay vertices is 80% for true decay lengths greater than 3mm, as estimated by the simulation. The efficiency falls at shorter decay length as it becomes harder to resolve the secondary vertex from the IP. The efficiency for reconstructing at least one secondary vertex is $\sim 50\%$ in b hemispheres, $\sim 15\%$ in charm hemispheres and $\sim 3\%$ in light quark hemispheres. The efficiency for reconstructing more than one secondary vertex is $\sim 5\%$ in b hemispheres. For hemispheres containing secondary vertices, the 'seed' vertex is chosen to be the one furthest from the IP. Vertices consistent with a $K^0_s \to \pi^+\pi^-$ decay are excluded from the seed vertex selection and the two tracks are discarded.

A vertex axis is formed by a straight line joining the IP to the seed vertex.

The 3-D distance of closest approach of a track to the vertex axis, T, and the distance from the IP along the vertex axis to this point, L, are calculated for all quality tracks. Tracks which are not directly associated with the seed vertex but which pass T$<$ 0.1 cm and L/D$>$ 0.3 (where D is the distance from the IP to the seed vertex) are added to the set of tracks in the seed vertex to form the candidate B decay vertex, containing tracks from both the B and cascade D decays [5]. The distance from the IP to the location determined by fitting this set of tracks to a common vertex is the reconstructed decay length. Since the purity of the B charge reconstruction is lower for decays close to the IP, where tracks are more likely to be wrongly assigned, decay lengths are required to be > 1 mm.

The lifetime measurement relies on the ability to separate B^+ and B^0 decays by making use of the vertex charge (total charge of tracks associated with the vertex). Monte Carlo studies show that the purity of the charge reconstruction is more likely to be eroded by losing tracks from the B decay chain through track selection inefficiencies and track mis-assignment than by gaining mis-assigned tracks originating from the primary or other background to the B decay. Furthermore, the decays that are missing some B tracks tend to have lower vertex mass as well as lower charge purity. Hence the vertex mass (calculated assuming the tracks to be pions) is required to be > 2 GeV/c^2. In addition, the mass distribution (see Fig. 1) shows that a large fraction of the charm and light flavor contamination is eliminated by this cut. A sample of 9719 candidate B decay vertices remains, with a mean track multiplicity of 5.0.

To improve the B hadron charge reconstruction, tracks that fail the initial

selection but have $p_T > 200$ MeV/c and $\sqrt{\sigma_{r\phi}^2 + \sigma_{rz}^2} < 700\,\mu$m, where $\sigma_{r\phi}$ (σ_{rz}) is the uncertainty in the track position in the $r\phi$ (rz) plane close to the IP, are considered as decay track candidates. The charge of any such track passing T$<$ 0.1 cm and L/D$>$ 0.3 is added to the B decay charge. On average, 0.5 tracks satisfy these criteria per b hemisphere.

Fig. 2 shows a comparison of the reconstructed charge between data and Monte Carlo. The charged sample consists of 6033 vertices with vertex charge equal to $\pm$ 1,2 or 3, while the neutral sample consists of 3665 vertices with charge equal to 0. Monte Carlo studies indicate that the charged sample is 97.8% pure in B hadrons consisting of 52.8% B^+, 32.1% B^0, 8.6% B_s^0, and 4.3% B baryons. (Charge conjugation is implied throughout this paper.) Similarly, the neutral sample is 98.3% pure in B hadrons consisting of 25.3% B^+, 52.9% B^0, 13.9% B_s^0 and 6.2% B baryons. The statistical precision of the measurement depends on the difference between the B^+ and B^0 contents of these samples.

The B^+ and B^0 lifetimes are extracted using a binned maximum likelihood fit to the decay length distributions of the vertices in the charged and neutral samples simultaneously (see Fig. 3). For each set of parameter values, Monte Carlo decay length distributions are obtained by reweighting entries from generated B^+ and B^0 decays in the original Monte Carlo decay length distributions with $W(t,\tau) = (\frac{1}{\tau}\ e^{-t/\tau})/(\frac{1}{\tau_{gen}}\ e^{-t/\tau_{gen}})$, where τ is the B^+ or B^0 lifetime, $\tau_{gen} = 1.55$ ps, and t is the proper time of each decay. The fit then compares the decay length distributions from the data with the reweighted Monte Carlo distributions over the range 1 mm to 25 mm. The

fit yields $\tau_{B^+} = 1.67 \pm 0.07$ ps, $\tau_{B^0} = 1.66 \pm 0.08$ ps, and $\tau_{B^+}/\tau_{B^0} = 1.01^{+0.09}_{-0.08}$ with a $\chi^2 = 90$ for 76 degrees of freedom.

Systematic uncertainties due to detector and physics modeling, as well as those related to the fitting procedure, are described below and summarized in Table 1. A discrepancy between data and simulation in the fraction of tracks passing a set of quality cuts [6] is corrected for by removing 4% of the tracks from the simulation. The uncertainty due to the track finding efficiency is conservatively estimated as the full difference between fits with and without this correction. The decay length distribution of the smaller neutral sample, and hence the measured B^0 lifetime, is perturbed more than the charged sample by this conservative estimate of the tracking efficiency uncertainty. The uncertainty due to tracking resolution is similarly taken to be the difference between fits before and after smearing and shifting the track impact parameters in the rz plane to account for residual VXD misalignments [6]. Smearing by $\sigma = 20\,\mu\mathrm{m}/\sin\theta$ and shifting by up to 20 μm is required to match the core of the impact parameter distribution observed in the data. No correction is required to the impact parameters in the $r\phi$ plane. We have also made cross checks by performing the lifetime fits for B decay candidates in different ϕ regions and different data taking time periods separately. The results are found to be consistent within statistics.

The physics modeling systematic uncertainties are determined as follows. The mean fragmentation energy $<x_E>$ of the B hadron [15] and the shape of the x_E distribution [16] are varied. Since the fragmentation is assumed to be identical for the B^+ and B^0 mesons, this uncertainty has little effect on the lifetime ratio. The four branching fractions for $B^+/B^0 \to \overline{D^0}/D^- X$ are

independently varied by twice the uncertainty in the current world average for $B \to \overline{D^0}/D^- X$ [12]. The average B^+ and B^0 decay multiplicities are varied by ± 0.3 tracks [17] in an anticorrelated manner. Uncertainties in the B_s^0 and B baryon lifetimes and production fractions mostly affect the B^0 lifetime since the neutral B_s^0 and B baryon are a more significant background for the B^0 decays (92% of the B baryons are neutral in our simulation). Production fractions of B^+ and B^0 are assumed to be equal. The systematic errors due to uncertainties in charm meson decay topology are estimated by modifying the simulated D decay charged multiplicity and K^0 production to match existing measurements [18]. The effect of uncertainties in the charmed hadron lifetimes, as well as in their momentum spectra in the B decay rest frame is found to be negligible.

The fitting uncertainties are determined by varying the bin size used in the decay length distributions, and by modifying the cuts on the minimum (0–2 mm) and maximum (12–25 mm) decay lengths used in the fit. Fit results are consistent within statistics for these variations, but a systematic error is conservatively assigned using the RMS variation of the results.

The final results for the topological analysis are $\tau_{B^+} = 1.67 \pm 0.07(\text{stat}) \pm 0.06(\text{syst})$ ps, $\tau_{B^0} = 1.66 \pm 0.08 \pm 0.08$ ps, and $\tau_{B^+}/\tau_{B^0} = 1.01^{+0.09}_{-0.08} \pm 0.05$.

We now describe the semileptonic analysis. The initial step in the event selection is to select electron and muon candidates using the measured track parameters as well as measurements from the LAC and WIC respectively (see Ref. [19] for further details). To enhance the fraction of $Z^0 \to b\bar{b}$ events with little loss in efficiency, lepton candidates are required to have $p > 2$ GeV/c and momentum transverse to the nearest jet > 0.4 GeV/c (jets are found

using the JADE algorithm [20] with $y_{cut} = 0.005$). These cuts yield a sample of $\sim 34,000$ event hemispheres, with an efficiency of $\sim 75\%$ for semileptonic B decays within $|\cos\theta| < 0.6$ determined from our Monte Carlo simulation.

The secondary vertex reconstruction proceeds separately for each event hemisphere containing a lepton, and uses a multi-pass algorithm that operates on those tracks that have at least one VXD hit and are not from identified γ conversions, or K_s^0 or Λ decays. Tracks are initially classified as primary unless their 3-D impact parameter significance with respect to the IP is $> 3.5\,\sigma$ and $p > 0.8$ GeV/c, in which case they are classified as secondary.

In the first pass, the hemisphere containing the lepton candidate is required to include no more than four secondary tracks (excluding the lepton) and a candidate D vertex is constructed using all such tracks (vertex cuts are defined below). The D trajectory, found from the D vertex and the total momentum vector of tracks included in the vertex, must intersect the lepton to form a valid one-prong B vertex solution. If this is successful, an attempt is made to form a two-prong B vertex by attaching one primary track to the lepton near the point of intersection. This first pass identifies 91% of the final candidates; 40% of these are then modified by attaching one or two primary tracks to the existing D vertex. In case of multiple solutions, we select the one with the largest number of tracks and if more than one still remains, we select that with the smallest impact parameter between the D trajectory and the lepton or two-prong B vertex. A second pass is performed if no first pass candidate is identified. Here, a search is made for solutions in which one secondary track makes a valid two-prong B vertex with the lepton, the

remaining secondary tracks form a D vertex, and the D trajectory intersects the B vertex. Multiple solutions are handled as described above.

The requirements to accept a D vertex are: number of tracks ≤ 4; D vertex charge $|Q_D| \leq 1$; mass < 1.98 GeV/c^2; distance from IP $> 4\,\sigma$ and < 2.5 cm; and vertex χ^2 (2,3,4 prongs) $< (4, 12, 20)$. The requirements to accept a B vertex are: $|Q_{\rm tot}| \leq 1$ and mass > 1.4 GeV/c^2 for B+D tracks; decay length > 0.08 cm and < 2.4 cm; and any non-lepton track has $p > 0.4$ GeV/c. The requirements for the D vertex to be linked to the B vertex are: signed distance between D and B vertices > 200 μm; for one-prong B vertices, the distance of closest approach of the D trajectory to the lepton $< (130, 100, 70)$ μm for (2, 3, 4) prong D vertices; for two-prong B vertices, the three-dimensional impact parameter of the D trajectory with respect to the B vertex < 200 μm.

The efficiency for reconstructing a semileptonic B decay is estimated from the simulation to be 24% for decays with an identified lepton within $|\cos\theta| < 0.6$. The charged topology consisting of two-prong B and three-prong D vertices has poor B^+ purity and is therefore excluded from the sample. The final sample is made up of 634 charged and 584 neutral semileptonic B decay candidates. The charged sample is composed of the following (B:D) track topologies: (1:2) and (1:4); the neutral sample is composed of (1:3), (2:2) and (2:4) topologies.

Monte Carlo studies show that the charged (neutral) sample is 97.4% (98.9%) pure in B hadrons with flavor contents of 66.6% B^+, 22.9% B^0, 5.5% B_s^0, and 2.4% B baryons for the charged sample, and 19.5% B^+, 60.2% B^0, 14.8% B_s^0, and 4.4% B baryons for the neutral sample. The fraction

of misidentified leptons is 7.0% (9.7%) for charged (neutral) candidates, as determined from the simulation. However, these are predominantly B decays with good charge purity.

As a check of the algorithm, the requirements on the charges of the B and D vertices are removed (for Figs. 4(a) and 4(b) only). Figure 4(a) shows that, as expected, the charges of the lepton and D vertex are opposite for most reconstructed decays with a charged D vertex. Furthermore, the charge distribution resulting from the lepton+slow transition pion vertex (from $D^{*(*)}$) shown in Fig. 4(b) indicates that the track combined with the lepton to form a two-prong B vertex most often has charge opposite that of the lepton, as expected for $B \to D^* l\nu$ and most $B \to D^{**} l\nu$ decays. Figure 4 also shows the total vertex momentum distribution, and the D vertex multiplicity distribution (with the nominal charge requirements on the vertices).

The B^+ and B^0 lifetimes are extracted from the decay length distributions (see Fig. 5) following the same procedure as for the topological analysis. The fit yields $\tau_{B^+} = 1.61^{+0.13}_{-0.12}$ ps, $\tau_{B^0} = 1.56^{+0.14}_{-0.13}$ ps and $\tau_{B^+}/\tau_{B^0} = 1.03^{+0.16}_{-0.14}$ with a $\chi^2 = 78$ for 76 degrees of freedom.

Systematic uncertainties are treated in the same way as described previously and are summarized in Table 1. Here we concentrate on uncertainties specific to the semileptonic analysis. In addition to the correction for the track finding efficiency, a 0.9^{m-2} correction to the vertex reconstruction efficiency is applied, where m is the D vertex track multiplicity. The B^0 lifetime is more sensitive to the track finding and resolution uncertainties than the B^+ lifetime because they affect the relative abundance of the various topolo-

gies, and the fraction of wrong-charge vertices at short decay length is higher for two-prong than for one-prong B vertex topologies. It was checked that the lifetimes obtained in four different ϕ regions are statistically consistent.

Sensitivity to the branching ratio for decays involving $b \to c \to l$ transitions or for $B \to \tau\nu_\tau X$ decays is negligible. Similarly, uncertainties due to the charm hadron lifetimes are negligible. A slight discrepancy between data and simulation is observed in the vertex total momentum distribution for the neutral sample (see Fig. 4(c)). This mismatch is investigated by reweighting the Monte Carlo D vertex momentum distribution to match the data in both charged and neutral samples. Although the discrepancy may be attributed in part to the B decay modeling, we conservatively assign an uncertainty to be the difference between fits with and without reweighting.

The final results for the semileptonic analysis are $\tau_{B^+} = 1.61^{+0.13}_{-0.12}(\text{stat}) \pm 0.07(\text{syst})$ ps, $\tau_{B^0} = 1.56^{+0.14}_{-0.13} \pm 0.10$ ps, and $\tau_{B^+}/\tau_{B^0} = 1.03^{+0.16}_{-0.14} \pm 0.09$.

In summary, from 150,000 Z^0 decays the B^+ and B^0 lifetimes have been measured using novel topological and semileptonic techniques. Combining the measurements from the two analyses, taking into account correlated statistical and systematic errors, yields the following SLD averages:

$$\begin{aligned} \tau_{B^+} &= 1.66 \pm 0.06(\text{stat}) \pm 0.05(\text{syst}) \text{ ps}, \\ \tau_{B^0} &= 1.64 \pm 0.08(\text{stat}) \pm 0.08(\text{syst}) \text{ ps}, \\ \tau_{B^+}/\tau_{B^0} &= 1.01 \pm 0.07(\text{stat}) \pm 0.06(\text{syst}). \end{aligned}$$

These results are consistent with the expectation that the B^+ and B^0 lifetimes are nearly equal and have a statistical accuracy among the best of the current measurements [2, 3, 4].

We thank the personnel of the SLAC accelerator department and the technical staffs of our collaborating institutions for their outstanding efforts.

References

[1] see for example, I.I. Bigi *et al.*, in *B Decays*, edited by S. Stone (World Scientific, New York, 1994), p. 132.

[2] D. Buskulic *et al.*, Z. Phys. **C71**, 31 (1996); P. Abreu *et al.*, Z. Phys. **C68**, 13 (1995), P. Abreu *et al.*, Report No. CERN-PPE/96-139, 1996; R. Akers *et al.*, Z. Phys. **C67**, 379 (1995); F. Abe *et al.*, Phys. Rev. Lett. **76**, 4462 (1996).

[3] F. Abe *et al.*, Phys. Rev. Lett. **72**, 3456 (1994).

[4] W. Adam *et al.*, Z. Phys. **C68**, 363 (1995).

[5] D. J. Jackson, Report No. SLAC-PUB-7215, 1996, to be published in *Nucl. Inst. and Meth.*

[6] K. Abe *et al.*, Phys. Rev. **D53**, 1023 (1996).

[7] T. Sjöstrand, Comp. Phys. Comm. **82**, 74 (1994).

[8] R. Brun *et al.*, Report No. CERN-DD/EE/84-1, 1989.

[9] C. Peterson *et al.*, Phys. Rev. **D27**, 105 (1983).

[10] B decay model provided by the CLEO Collaboration.

[11] B. Barish *et al.*, Phys. Rev. Lett. **76**, 1570 (1996); H. Albrecht *et al.*, Z. Phys. **C58**, 191 (1993); H. Albrecht *et al.*, Z. Phys. **C62**, 371 (1994); M. Thulasidas, Ph.D thesis, Syracuse University, 1993; G. Crawford

et al., Phys. Rev. **D45**, 752 (1992); D. Bortoletto *et al.*, Phys. Rev. **D45**, 21 (1992).

[12] F. Muheim, in *Proceedings of the 8th Meeting Division of Particles and Fields, Albuquerque, August, 1994* (World Scientific, New York, 1995), Vol. 1, p. 851.

[13] N. Isgur, D. Scora, B. Grinstein, and M.B. Wise, Phys. Rev. **D39**, 799 (1989).

[14] Particle Data Group, Phys. Rev. **D50**, Part I (1994).

[15] see for example, R. Akers *et al.*, Z. Phys. **C60**, 601 (1993); D. Buskulic *et al.*, Z. Phys. **C62**, 179 (1994); P. Abreu *et al.*, Z. Phys. **C66**, 323 (1995).

[16] M. G. Bowler, Z. Phys. **C11**, 169 (1981).

[17] H.Albrecht *et al.*, Z. Phys. **C54**, 13 (1992); R.Giles *et al.*, Phys. Rev. **D30**, 2279 (1984).

[18] D.Coffman *et al.*, Phys. Lett. **B263**, 135 (1991).

[19] K. Abe *et al.*, Phys. Rev. Lett. **74**, 2895 (1995).

[20] S. Bethke *et al.*, Phys. Lett. **213B**, 235 (1988).

Table 1: Summary of systematic uncertainties in the B^+ and B^0 lifetimes and their ratio.

Systematic Error		Topological analysis			Semileptonic analysis		
		$\Delta\tau_{B^+}$ (ps)	$\Delta\tau_{B^0}$ (ps)	$\Delta\frac{\tau_{B^+}}{\tau_{B^0}}$	$\Delta\tau_{B^+}$ (ps)	$\Delta\tau_{B^0}$ (ps)	$\Delta\frac{\tau_{B^+}}{\tau_{B^0}}$
				Detector Modeling			
Tracking efficiency		0.011	0.035	0.028	0.017	0.029	0.023
Tracking resolution		0.012	0.011	0.010	0.020	0.030	0.033
Lepton misidentif.	$\pm$ 25%	na	na	na	$\pm$0.006	$\pm$0.007	$<$0.003
				Physics Modeling			
b fragmentation	$\langle x_E \rangle = 0.700 \pm 0.011$	$\mp$0.034	$\mp$0.034	$<$0.003	$\mp$0.025	$\mp$0.039	$\pm$0.010
	Ref.[16]	$+$0.008	$+$0.015	$-$0.005	$+$0.024	$+$0.003	$+$0.012
BR($B \to DX$)	Ref.[12]	0.010	0.012	0.010	0.008	0.006	0.010
BR($B \to D\overline{D}X$)	0.15 $\pm$ 0.05	0.006	0.006	0.006	0.009	0.008	0.011
$\frac{BR(B\to D^{**}l\nu)}{BR(B\to Xl\nu)}$	0.230 $\pm$ 0.115	na	na	na	$\pm$0.011	$\mp$0.018	$\pm$0.016
B decay multiplicity	5.3 $\pm$ 0.3	0.016	0.012	0.003	na	na	na
B_s^0 fraction	0.115 $\pm$ 0.040	$\pm$0.012	$\pm$0.004	$\pm$0.005	$\pm$0.007	$\mp$0.007	$\pm$0.009
B baryon fraction	0.072 $\pm$ 0.040	$\pm$0.013	$\pm$0.039	$\mp$0.017	$\pm$0.008	$\pm$0.016	$\mp$0.006
B_s^0 lifetime	1.55 $\pm$ 0.10 ps	$<$0.003	$\mp$0.025	$\pm$0.016	$\pm$0.003	$\mp$0.028	$\pm$0.020
B baryon lifetime	1.10 $\pm$ 0.08 ps	$<$0.003	$\pm$0.006	$\pm$0.004	$<$0.003	$\mp$0.007	$\pm$0.005
D decay multiplicity	Ref.[18]	$-$0.011	$+$0.006	$-$0.010	$+$0.014	$+$0.009	$<$0.003
D decay K^0 yield	Ref.[18]	$-$0.005	$-$0.020	$+$0.010	$<$0.003	$<$0.003	$<$0.003
D mom. mismatch		na	na	na	$<$0.003	$-$0.034	$+$0.022
				Monte Carlo and Fitting			
Fitting systematics		0.024	0.013	0.022	0.037	0.052	0.061
MC statistics		0.012	0.013	0.015	0.023	0.024	0.027
TOTAL		0.055	0.078	0.050	0.066	0.097	0.088

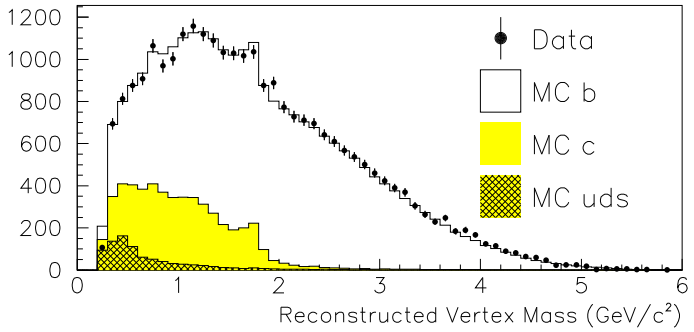

Figure 1: Mass of reconstructed vertex for data (points) and Monte Carlo (histogram) in topological analysis.

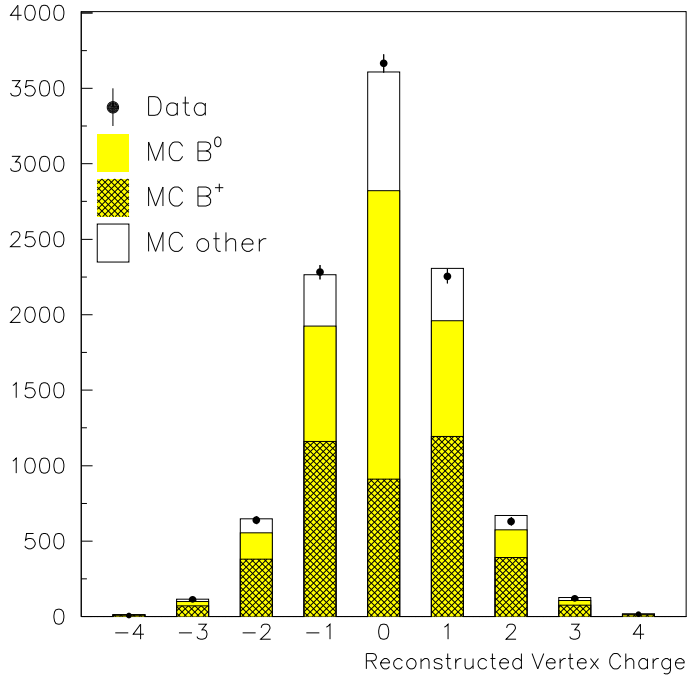

Figure 2: Reconstructed vertex charge for data (points) and Monte Carlo (histogram) in topological analysis.

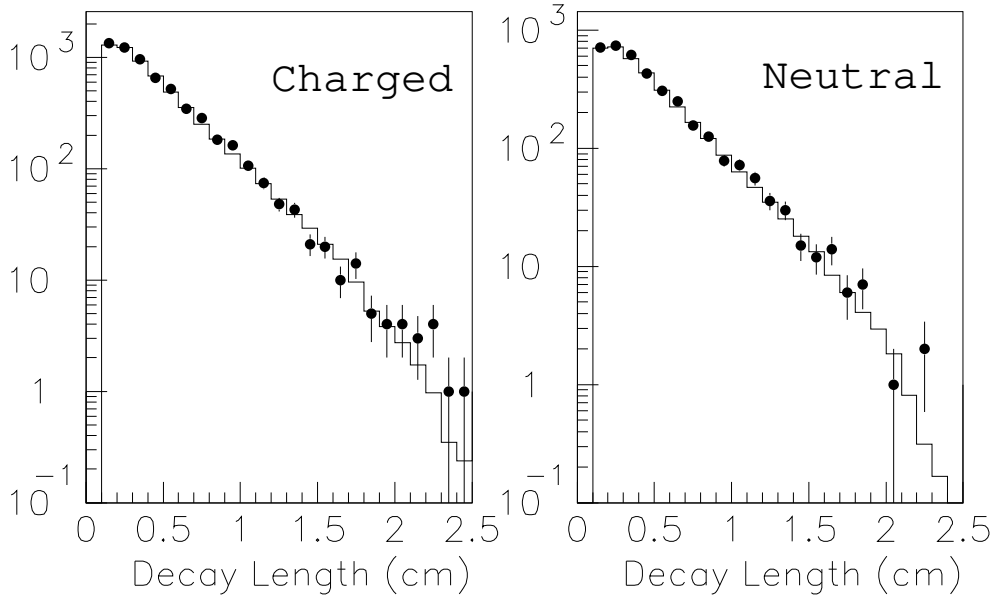

Figure 3: Decay length distributions for data (points) and best fit Monte Carlo (histogram) in topological analysis.

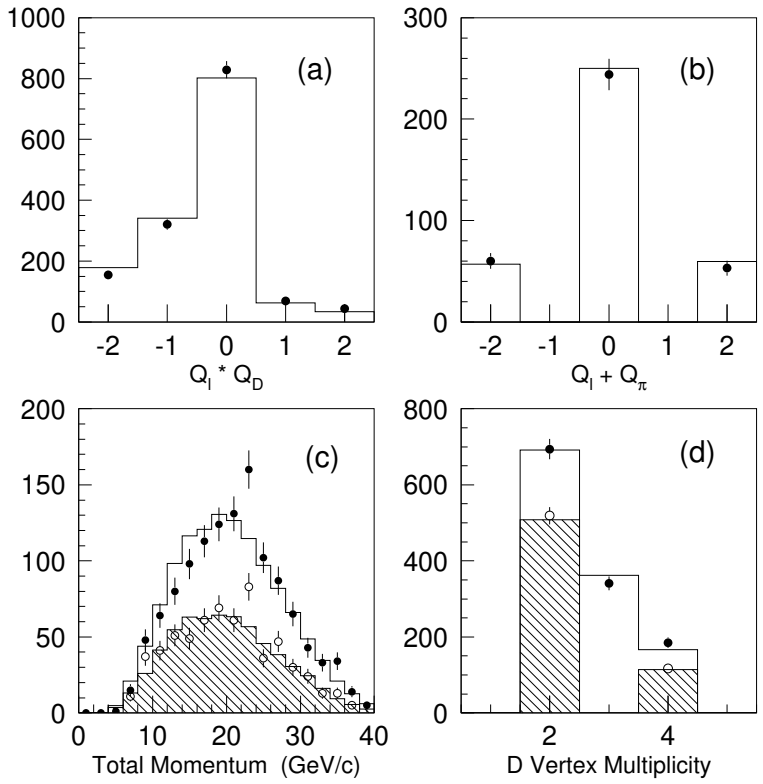

Figure 4: Distributions of (a) the product of lepton and D-vertex charges, (b) sum of lepton and slow transition pion charges for data (points) and Monte Carlo (histograms) with no charge requirement at the B and D vertices. Distributions of (c) total momentum of the B+D tracks and (d) D vertex multiplicity for data (solid circles are for total sample, open circles are for charged sample only) and Monte Carlo (histograms are for total sample, shaded portions are for charged sample only).

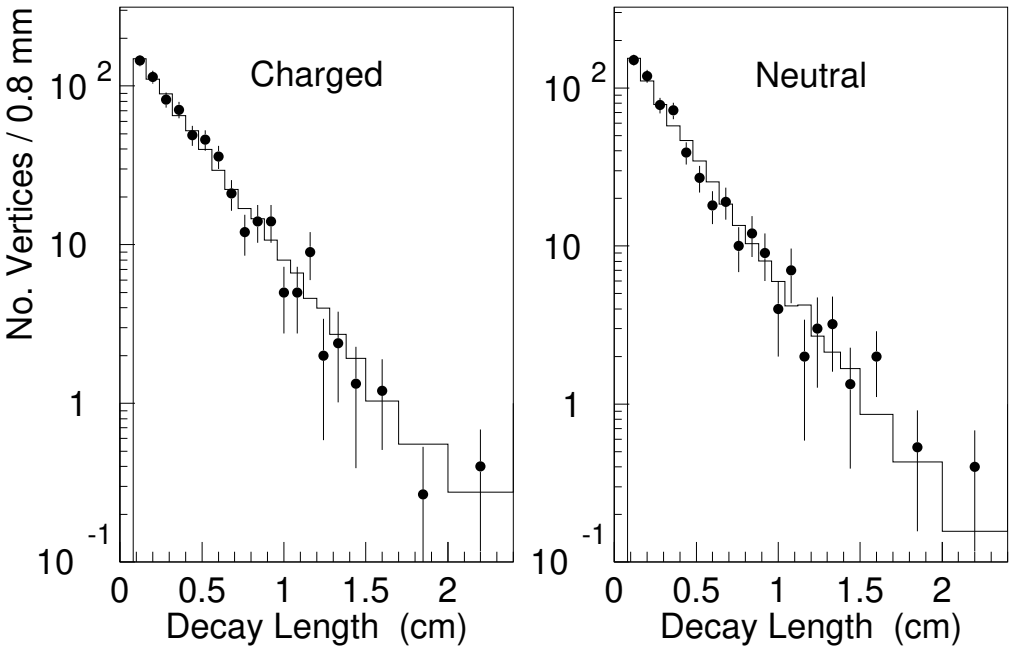

Figure 5: Decay length distributions for data (points) and best fit Monte Carlo (histogram) in the semileptonic analysis.